

Electronic Supplementary Information:

Intramolecular OH... π Interactions in Alkenols and Alkynols

Benjamin J. Miller,[†] Joseph R. Lane,[‡] and Henrik G. Kjaergaard^{*,¶}

Department of Chemistry, University of Otago, P.O. Box 56, Dunedin, New Zealand, Department of Chemistry, University of Waikato, Private Bag 3105, Hamilton 3240, New Zealand, and Department of Chemistry, University of Copenhagen, Universitetsparken 5, DK-2100 Copenhagen Ø, Denmark

E-mail: hgk@chem.ku.dk

*To whom correspondence should be addressed

[†]Department of Chemistry, University of Otago, P.O. Box 56, Dunedin, New Zealand

[‡]Department of Chemistry, University of Waikato, Private Bag 3105, Hamilton 3240, New Zealand

[¶]Department of Chemistry, University of Copenhagen, Universitetsparken 5, DK-2100 Copenhagen Ø, Denmark

Table SI: Calculated local mode parameters (cm^{-1}) for the conformers of **PA**, **AA**, **PC** and **AC** obtained from CCSD(T)-F12/VDZ-F12 potential energy curves.

Conformer	$\tilde{\omega}$	$\tilde{\omega}_x$
PA1	3844.10	85.76
PA2	3846.92	85.84
AA1	3837.32	86.45
AA2	3834.80	86.66
AA3	3868.38	85.84
AA4	3855.52	86.36
PC1	3809.90	86.70
PC2	3862.07	85.92
PC3	3847.68	86.66
PC4	3863.96	86.01
PC5	3841.68	86.81
AC1	3804.30	87.65
AC2	3827.81	86.47
AC3	3862.08	86.21
AC4	3859.22	86.33
AC5	3845.25	86.74

Table SII: Expansion coefficients of the CCSD(T)-F12a/VDZ-F12 dipole moment function of propargyl alcohol

μ_i	PA1			PA2		
	μ_x	μ_y	μ_z	μ_x	μ_y	μ_z
$\mu_0(D)$	1.01883	-0.56061	0.86018	0.00000	-1.68616	-0.79637
$\mu_1(D/\text{\AA})$	0.50364	0.61826	0.10351	0.00000	-0.02346	-0.75474
$\mu_2(D/\text{\AA}^2)$	-0.47076	-0.76223	0.07984	0.00000	-0.10830	1.16750
$\mu_3(D/\text{\AA}^3)$	-0.81947	-0.62575	-0.35159	0.00000	0.35132	1.16327
$\mu_4(D/\text{\AA}^4)$	-0.09781	-0.14190	-0.02517	0.00000	-0.05214	0.06122
$\mu_5(D/\text{\AA}^5)$	0.30558	0.35390	0.03855	0.00000	-0.04434	-0.73146
$\mu_6(D/\text{\AA}^6)$	0.00957	0.01638	-0.01711	0.00000	-0.00120	0.06789

Table SIII: Expansion coefficients of the CCSD(T)-F12a/VDZ-F12 dipole moment function of allyl alcohol

μ_i	AA1			AA2		
	μ_x	μ_y	μ_z	μ_x	μ_y	μ_z
$\mu_0(D)$	-0.05486	-0.26154	-1.62268	-0.99245	-1.16590	0.20738
$\mu_1(D/\text{\AA})$	0.66908	0.00156	-0.12915	-0.51399	0.22448	-0.33370
$\mu_2(D/\text{\AA}^2)$	-0.98993	-0.06125	-0.01055	0.64104	-0.48647	0.49254
$\mu_3(D/\text{\AA}^3)$	-0.95508	0.03151	0.49975	0.96214	-0.12973	0.48855
$\mu_4(D/\text{\AA}^4)$	-0.08179	0.01048	0.00331	0.08718	-0.08347	0.05645
$\mu_5(D/\text{\AA}^5)$	0.55466	0.04449	-0.08924	-0.47186	0.21487	-0.26364
$\mu_6(D/\text{\AA}^6)$	0.03419	-0.01402	0.00369	-0.06367	0.07392	-0.03864
μ_i	AA3			AA4		
	μ_x	μ_y	μ_z	μ_x	μ_y	μ_z
$\mu_0(D)$	0.00000	0.22696	1.76624	-1.19583	1.10226	0.10621
$\mu_1(D/\text{\AA})$	0.00000	0.73837	0.30150	0.09627	0.45302	0.50545
$\mu_2(D/\text{\AA}^2)$	0.00000	-1.12364	-0.22488	-0.39232	-0.67447	-1.03208
$\mu_3(D/\text{\AA}^3)$	0.00000	-1.10760	-0.70542	0.01712	-0.95122	-0.90762
$\mu_4(D/\text{\AA}^4)$	0.00000	-0.17428	-0.03982	-0.03109	-0.01328	-0.04874
$\mu_5(D/\text{\AA}^5)$	0.00000	0.65619	0.23592	0.14755	0.50315	0.64494
$\mu_6(D/\text{\AA}^6)$	0.00000	0.04858	0.02951	0.00103	0.02140	0.03506

Table SIV: Expansion coefficients of the CCSD(T)-F12a/VDZ-F12 dipole moment function of propargyl carbinol

	PC1			PC2		
μ_i	μ_x	μ_y	μ_z	μ_x	μ_y	μ_z
$\mu_0(D)$	-1.14389	-0.84257	0.40173	0.00000	1.43145	0.16526
$\mu_1(D/\text{Å})$	0.11438	-0.02433	0.76150	0.00000	0.64914	-0.50374
$\mu_2(D/\text{Å}^2)$	-0.45818	-0.47861	-0.48522	0.00000	-0.71963	1.00312
$\mu_3(D/\text{Å}^3)$	-0.07748	-0.13699	-0.77279	0.00000	-1.14720	0.65961
$\mu_4(D/\text{Å}^4)$	-0.05482	-0.05365	-0.05950	0.00000	-0.10497	0.13746
$\mu_5(D/\text{Å}^5)$	0.15181	0.19977	0.11959	0.00000	-0.48617	-0.38231
$\mu_6(D/\text{Å}^6)$	0.05009	0.11954	-0.09206	0.00000	-0.02200	-0.23177
	PC3			PC4		
μ_i	μ_x	μ_y	μ_z	μ_x	μ_y	μ_z
$\mu_0(D)$	1.24159	-0.43380	0.34015	-1.18764	0.88504	-1.25525
$\mu_1(D/\text{Å})$	0.053218	-0.10136	-0.53848	0.15158	0.78471	-0.13170
$\mu_2(D/\text{Å}^2)$	-0.61081	0.18494	0.85905	-0.49796	-1.03526	0.23750
$\mu_3(D/\text{Å}^3)$	-1.01189	0.30443	0.56869	-0.07268	-1.27706	0.38568
$\mu_4(D/\text{Å}^4)$	-0.08834	-0.02182	0.12014	-0.06782	-0.14525	0.05835
$\mu_5(D/\text{Å}^5)$	0.47031	-0.13731	-0.35917	0.20823	0.66893	-0.29860
$\mu_6(D/\text{Å}^6)$	0.10039	-0.01771	-0.18632	-0.01398	0.06341	0.01888
	PC5					
μ_i	μ_x	μ_y	μ_z			
$\mu_0(D)$	0.00158	-1.30971	-1.40162			
$\mu_1(D/\text{Å})$	0.65886	-0.06868	-0.21436			
$\mu_2(D/\text{Å}^2)$	-1.02375	-0.01806	0.20436			
$\mu_3(D/\text{Å}^3)$	-0.99114	0.38818	0.49290			
$\mu_4(D/\text{Å}^4)$	-0.08030	-0.02506	0.03186			
$\mu_5(D/\text{Å}^5)$	0.63024	-0.07642	-0.51232			
$\mu_6(D/\text{Å}^6)$	0.07271	-0.05111	0.42196			

Table SV: Expansion coefficients of the CCSD(T)-F12a/VDZ-F12 dipole moment function of allyl carbinol

	AC1			AC2		
μ_i	μ_x	μ_y	μ_z	μ_x	μ_y	μ_z
$\mu_0(D)$	-1.42772	0.37286	1.00894	1.31716	0.43376	1.21767
$\mu_1(D/\text{\AA})$	-0.20369	0.76417	0.14150	-0.11171	0.61613	0.42298
$\mu_2(D/\text{\AA}^2)$	-0.72270	-0.48616	0.11664	0.71878	-0.41717	0.15523
$\mu_3(D/\text{\AA}^3)$	-0.19605	-0.61948	-0.17925	0.25646	-0.65180	-0.20923
$\mu_4(D/\text{\AA}^4)$	-0.03539	-0.02130	0.01940	0.03807	0.14433	0.01278
$\mu_5(D/\text{\AA}^5)$	0.33709	0.21312	0.00284	-0.031233	0.77524	-0.06785
$\mu_6(D/\text{\AA}^6)$	0.18213	-0.24547	-0.06074	-0.01279	-1.30505	-0.21444
	AC3			AC4		
μ_i	μ_x	μ_y	μ_z	μ_x	μ_y	μ_z
$\mu_0(D)$	1.21448	-0.75446	-0.83180	1.21941	0.32925	0.80653
$\mu_1(D/\text{\AA})$	0.54219	-0.37730	0.38562	0.54297	-0.49265	0.03934
$\mu_2(D/\text{\AA}^2)$	-0.66507	0.67189	-0.83508	-0.71915	1.11648	0.08516
$\mu_3(D/\text{\AA}^3)$	-1.03150	0.75064	-0.52108	-1.07522	0.82412	-0.17169
$\mu_4(D/\text{\AA}^4)$	-0.07665	0.07467	-0.09156	-0.07657	0.09649	0.01306
$\mu_5(D/\text{\AA}^5)$	0.46896	-0.41259	0.50160	0.50683	-0.63970	-0.00972
$\mu_6(D/\text{\AA}^6)$	0.09674	-0.05949	-0.08823	0.11197	-0.02459	0.04319
	AC5					
μ_i	μ_x	μ_y	μ_z			
$\mu_0(D)$	-0.15262	1.24337	-0.80867			
$\mu_1(D/\text{\AA})$	0.05183	-0.27146	-0.62175			
$\mu_2(D/\text{\AA}^2)$	-0.03124	0.54720	0.92670			
$\mu_3(D/\text{\AA}^3)$	-0.02369	0.10854	1.13230			
$\mu_4(D/\text{\AA}^4)$	-0.03008	0.07329	0.02845			
$\mu_5(D/\text{\AA}^5)$	0.04630	-0.09012	-0.55600			
$\mu_6(D/\text{\AA}^6)$	-0.03619	0.52120	0.19009			

Table SVI: Anharmonic oscillator calculated OH-stretching transitions (in cm^{-1} and f) for propargyl alcohol.^a

$\Delta\nu_{\text{OH}}$	PA1		PA1	
	$\tilde{\nu}$	f	$\tilde{\nu}$	f
1	3672	4.49×10^{-6}	3678	3.72×10^{-6}
2	7174	4.93×10^{-7}	7184	6.19×10^{-7}
3	10503	1.98×10^{-8}	10519	2.67×10^{-8}
4	13661	1.10×10^{-9}	13682	1.41×10^{-9}
5	16648	9.82×10^{-10}	16673	1.14×10^{-10}

^aCalculated with the CCSD(T)-F12a/VDZ-F12 method, not including relative abundance.

Table SVII: Anharmonic oscillator calculated OH-stretching transitions (in cm^{-1} and f) for allyl alcohol.^a

$\Delta\nu_{\text{OH}}$	AA1		AA2		AA3		AA4	
	$\tilde{\nu}$	f	$\tilde{\nu}$	f	$\tilde{\nu}$	f	$\tilde{\nu}$	f
1	3664	3.07×10^{-6}	3661	2.81×10^{-6}	3697	4.21×10^{-6}	3683	2.92×10^{-6}
2	7156	4.69×10^{-7}	7150	4.32×10^{-7}	7222	6.35×10^{-7}	7193	6.41×10^{-7}
3	10475	2.04×10^{-8}	10464	1.78×10^{-8}	10575	2.49×10^{-8}	10530	2.80×10^{-8}
4	13620	1.14×10^{-9}	13606	9.41×10^{-10}	13757	1.22×10^{-9}	13695	1.45×10^{-9}
5	16593	9.95×10^{-11}	16574	8.11×10^{-11}	16767	9.45×10^{-11}	16687	1.17×10^{-10}

^aCalculated with the CCSD(T)-F12a/VDZ-F12 method, not including relative abundance.

Table SVIII: Anharmonic oscillator calculated OH-stretching transitions (in cm^{-1} and f) for propargyl carbinol.^a

$\Delta\nu_{\text{OH}}$	PC1		PC2		PC3		PC4		PC5	
	$\tilde{\nu}$	f								
1	3636	4.38×10^{-6}	3690	4.45×10^{-6}	3674	3.88×10^{-6}	3692	4.34×10^{-6}	3668	3.17×10^{-6}
2	7100	3.63×10^{-7}	7209	6.98×10^{-7}	7175	5.69×10^{-7}	7212	6.57×10^{-7}	7162	5.11×10^{-7}
3	10389	1.60×10^{-8}	10555	2.87×10^{-8}	10503	2.38×10^{-8}	10560	2.60×10^{-8}	10483	2.16×10^{-8}
4	13506	9.90×10^{-10}	13730	1.51×10^{-9}	13658	1.28×10^{-9}	13736	1.28×10^{-9}	13630	1.13×10^{-9}
5	16448	9.28×10^{-11}	16733	1.23×10^{-10}	16639	1.09×10^{-10}	16740	1.00×10^{-10}	16604	9.49×10^{-11}

^aCalculated with the CCSD(T)-F12a/VDZ-F12 method, not including relative abundance.

Table SIX: Anharmonic oscillator calculated OH-stretching transitions (in cm^{-1} and f) for allyl carbinol.^a

$\Delta\nu_{\text{OH}}$	AC1		AC2		AC3		AC4		AC5	
	$\tilde{\nu}$	f								
1	3629	4.98×10^{-6}	3655	4.31×10^{-6}	3690	3.76×10^{-6}	3687	3.40×10^{-6}	3672	3.00×10^{-6}
2	7083	3.17×10^{-7}	7137	3.11×10^{-7}	7207	6.81×10^{-7}	7200	6.96×10^{-7}	7170	5.17×10^{-7}
3	10361	1.51×10^{-8}	10446	1.47×10^{-8}	10552	2.76×10^{-8}	10542	2.97×10^{-8}	10495	2.25×10^{-8}
4	13464	9.62×10^{-10}	13582	8.59×10^{-10}	13724	1.36×10^{-9}	13710	1.54×10^{-9}	13646	1.28×10^{-9}
5	16392	9.09×10^{-11}	16545	7.81×10^{-11}	16724	1.05×10^{-10}	16706	1.24×10^{-10}	16624	1.07×10^{-10}

^aCalculated with the CCSD(T)-F12a/VDZ-F12 method, not including relative abundance.

Acetylnic CH-stretching transitions

Studies on acetylnic CH-stretching overtone transitions are sparse. One study lists the $\Delta\nu_{\text{CH}} = 1$ and 2 transitions at 3330 cm^{-1} and 6565 cm^{-1} , respectively.¹ Local mode parameters can be obtained via a Birge-Sponer plot for these CH-stretching positions. Having obtained the local mode parameters it was possible to estimate where the higher overtones of the acetylnic CH-stretch should absorb. The $\Delta\nu_{\text{CH}} = 4, 5$ and 6 transitions of the acetylnic CH-stretch should be around $12750, 15700$ and 18555 cm^{-1} , respectively. As such, this group is not expected to be observable in the $\Delta\nu_{\text{OH}} = 4$ and 5 regions.

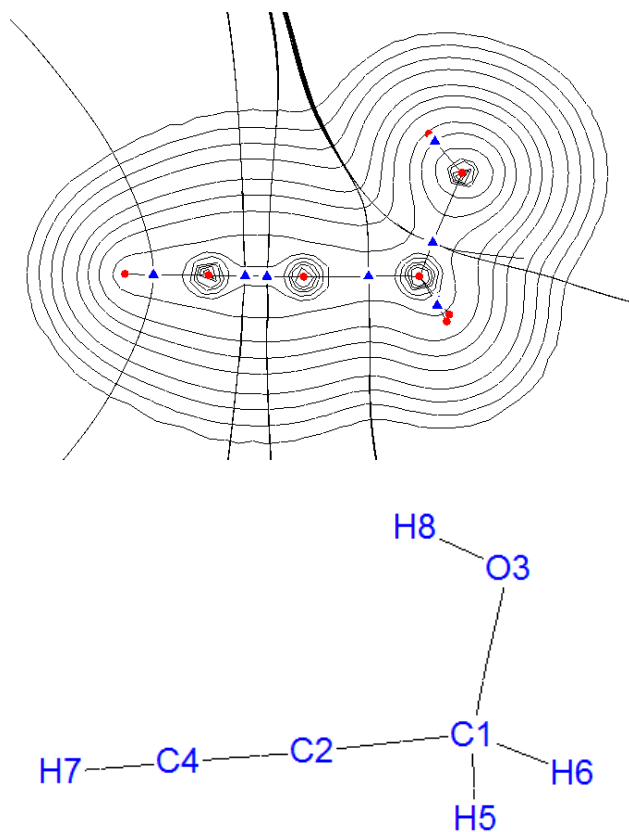


Figure SI: A 2D representation of the electron density of **PA1** calculated with the CCSD(T)-F12a/VDZ-F12 method. The electron density is represented on a plane passing through O3, C1 and C2. Red circles indicate atom positions, blue triangles indicate positions of (3,-1) bond critical points.

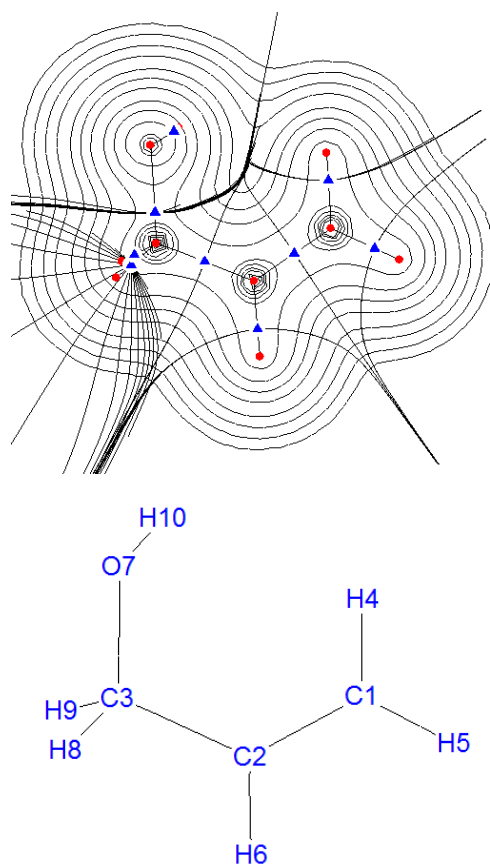


Figure SII: A 2D representation of the electron density of **AA1** calculated with the CCSD(T)-F12a/VDZ-F12 method. The electron density is represented on a plane passing through C3, C2 and C1. Red circles indicate atom positions, blue triangles positions of (3,-1) bond critical points.

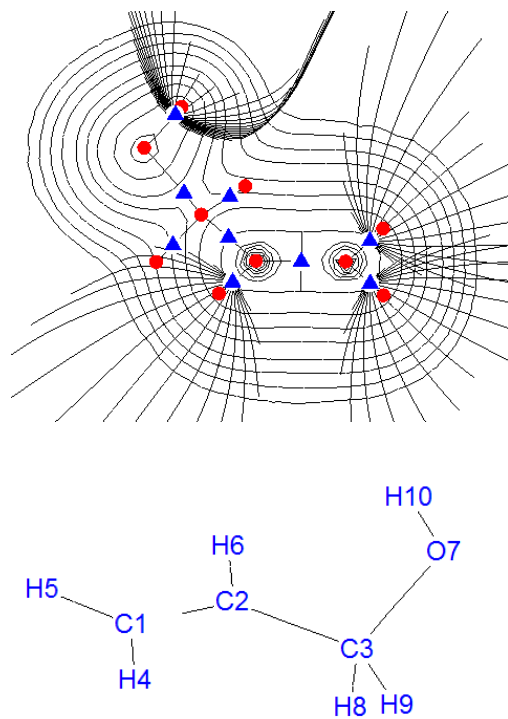


Figure SIII: A 2D representation of the electron density of **AA2** calculated with the CCSD(T)-F12a/VDZ-F12 method. The electron density is represented on a plane passing through C1, C2 and H10. Red circles indicate atom positions, blue triangles indicate positions of (3,-1) bond critical points.

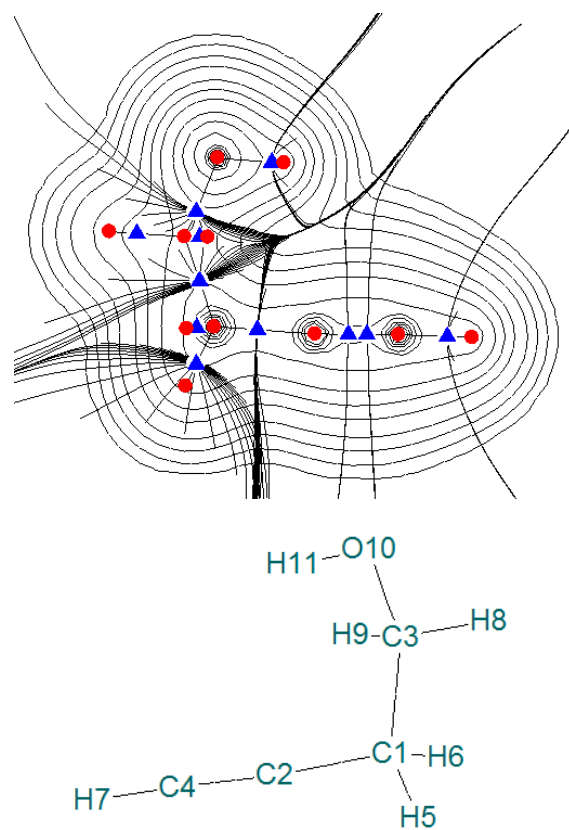


Figure SIV: A 2D representation of the electron density of **PC1** calculated with the CCSD(T)-F12a/VDZ-F12 method. The electron density is represented on a plane passing through C2, C4 and H11. Red circles indicate atom positions, blue triangles indicate positions of (3,-1) bond critical points.

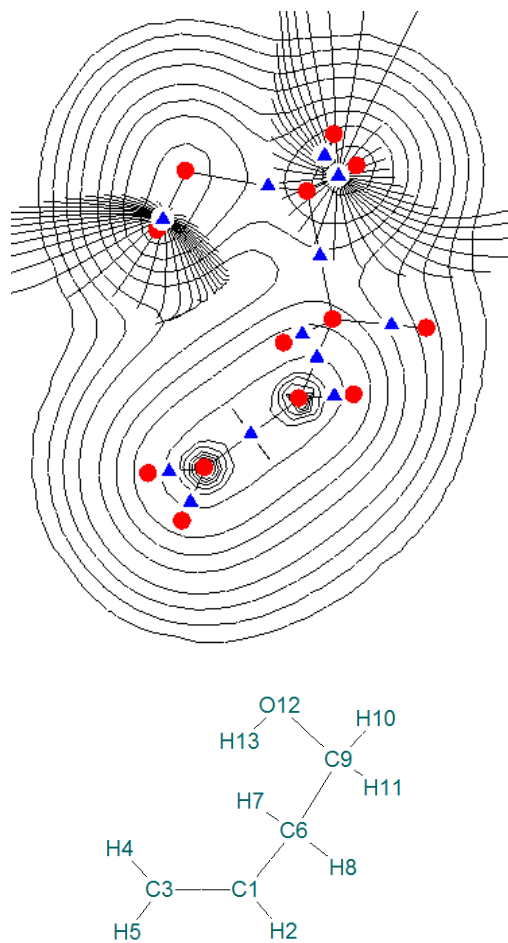


Figure SV: A 2D representation of the electron density of **AC1** calculated with the CCSD(T)-F12a/VDZ-F12 method. The electron density is represented on a plane passing through C1, C3 and H13. Red circles indicate atom positions, blue triangles indicate positions of (3,-1) bond critical points.

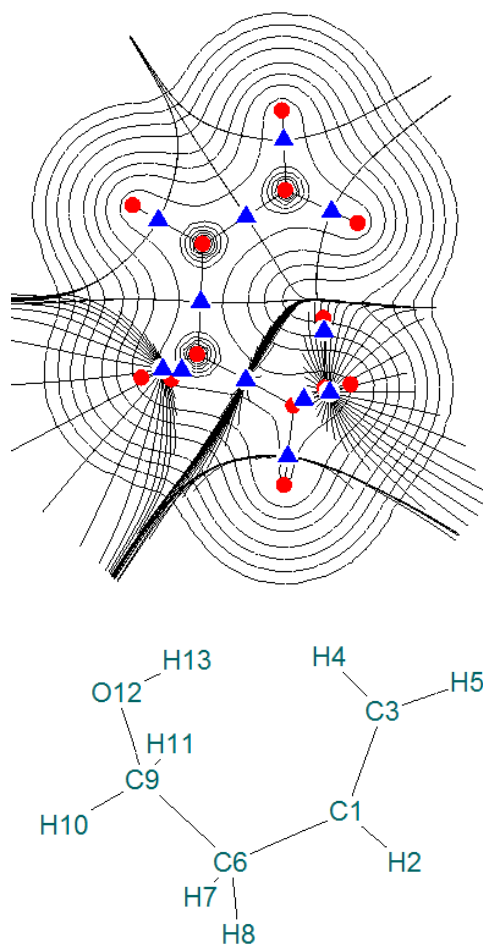


Figure S16: A 2D representation of the electron density of **AC2** calculated with the CCSD(T)-F12a/VDZ-F12 method. The electron density is represented on a plane passing through C1, C3 and C6. Red circles indicate atom positions, blue triangles indicate positions of (3,-1) bond critical points.

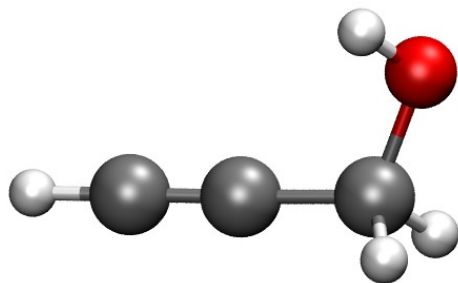
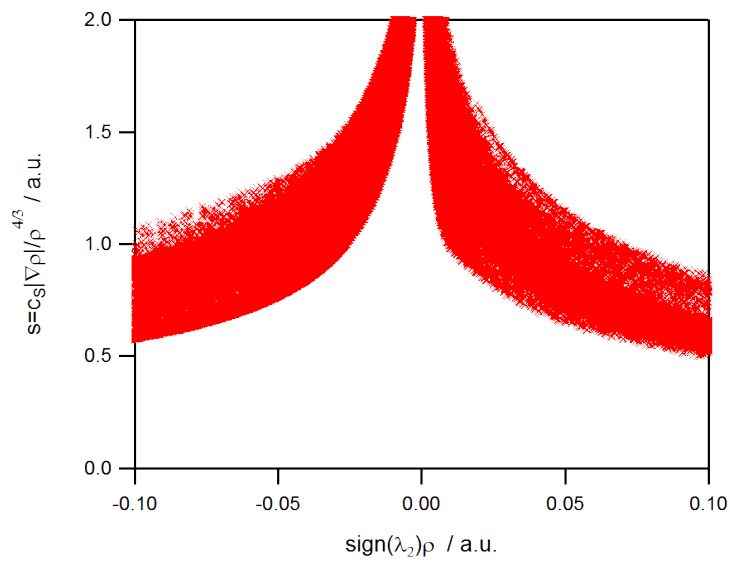


Figure SVII: Top - NCI plot of the reduced density gradient versus the electron density multiplied by the sign of the second Hessian eigenvalue for **PA1**. Bottom - NCI isosurface for **PA1** generated for $s=0.5$ a.u. with a blue-green-red color scale according to the values of $\text{sign}(\lambda_2)\rho$ from -0.05 to +0.05 a.u.

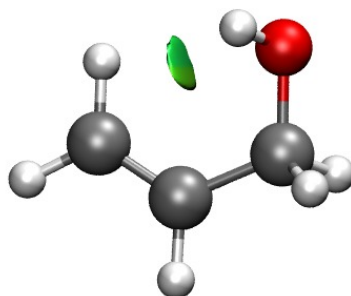
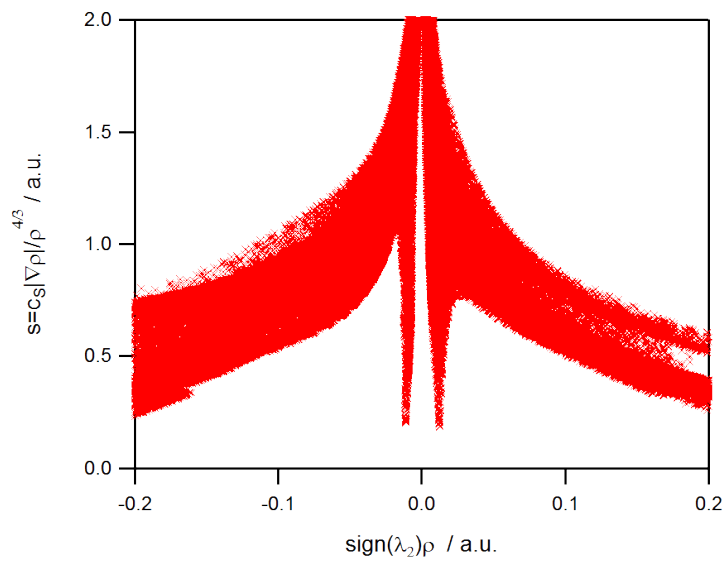


Figure SVIII: Top - NCI plot of the reduced density gradient versus the electron density multiplied by the sign of the second Hessian eigenvalue for **AA1**. Bottom - NCI isosurface for **AA1** generated for $s=0.5$ a.u. with a blue-green-red color scale according to the values of $\text{sign}(\lambda_2)\rho$ from -0.05 to $+0.05$ a.u.

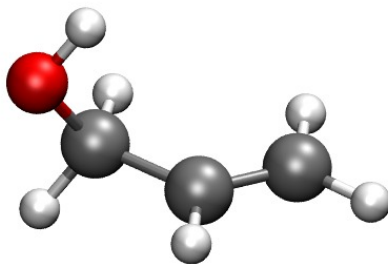
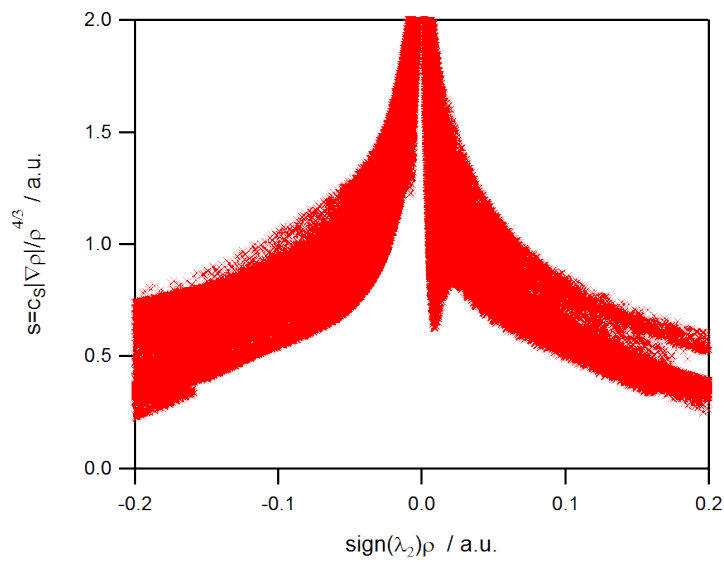


Figure SIX: Top - NCI plot of the reduced density gradient versus the electron density multiplied by the sign of the second Hessian eigenvalue for **AA2**. Bottom - NCI isosurface for **AA2** generated for $s=0.5$ a.u. with a blue-green-red color scale according to the values of $\text{sign}(\lambda_2)\rho$ from -0.05 to +0.05 a.u.

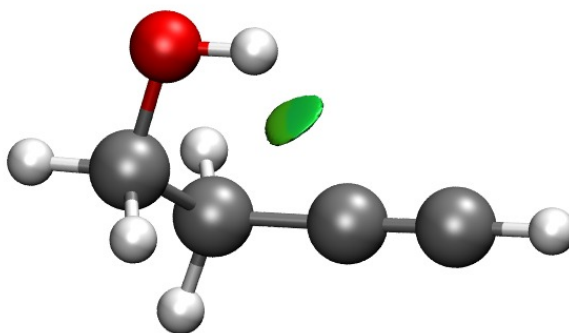
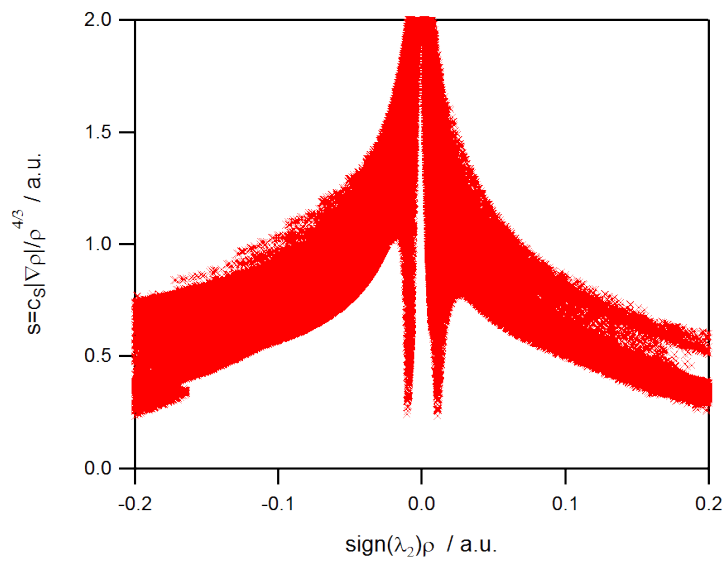


Figure SX: Top - NCI plot of the reduced density gradient versus the electron density multiplied by the sign of the second Hessian eigenvalue for **PC1**. Bottom - NCI isosurface for **PC1** generated for $s=0.5$ a.u. with a blue-green-red color scale according to the values of $\text{sign}(\lambda_2) \rho$ from -0.05 to +0.05 a.u.

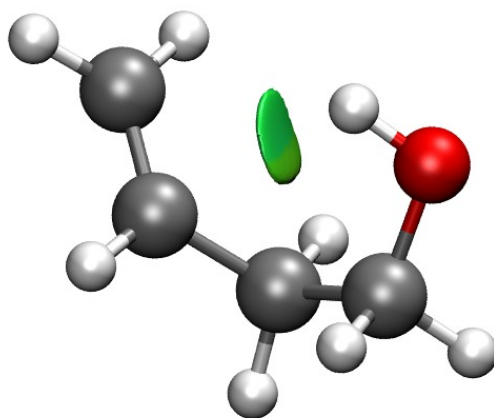
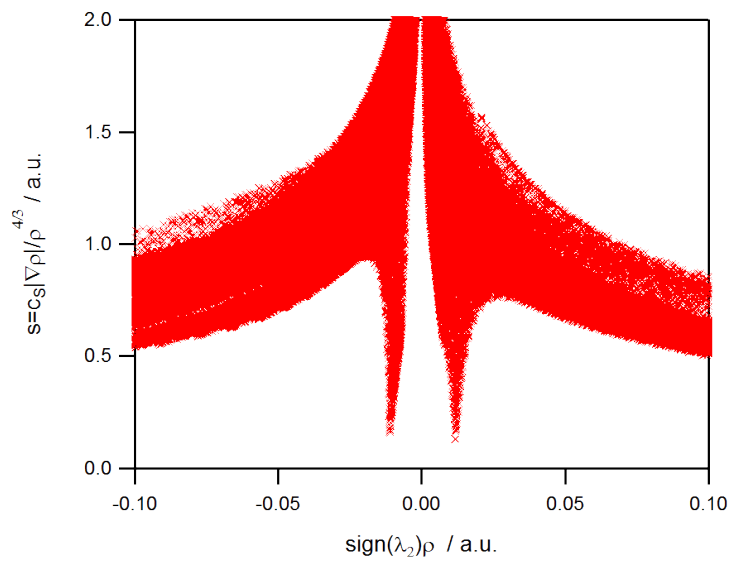


Figure SXI: Top - NCI plot of the reduced density gradient versus the electron density multiplied by the sign of the second Hessian eigenvalue for **AC1**. Bottom - NCI isosurface for **AC1** generated for $s=0.5$ a.u. with a blue-green-red color scale according to the values of $\text{sign}(\lambda_2)\rho$ from -0.05 to $+0.05$ a.u.

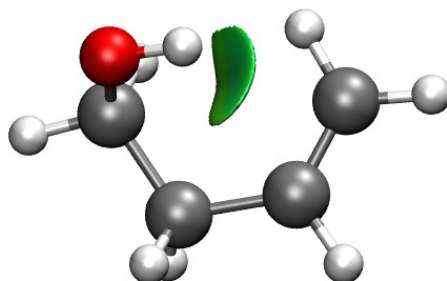
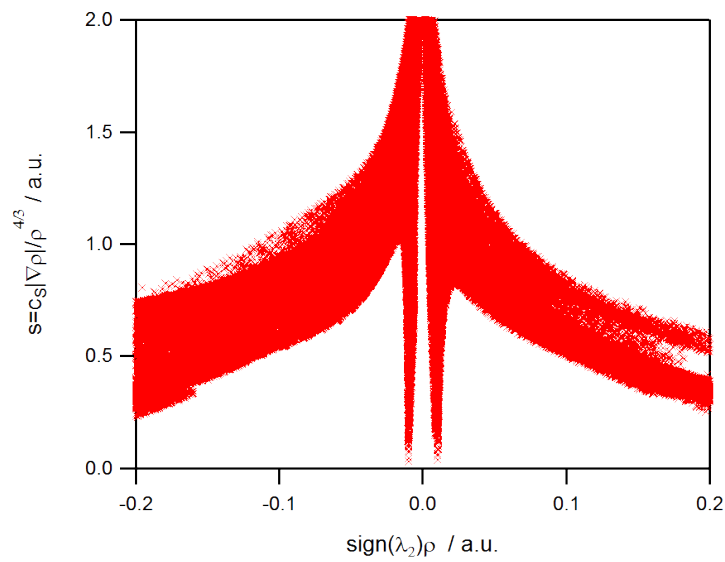


Figure SXII: Top - NCI plot of the reduced density gradient versus the electron density multiplied by the sign of the second Hessian eigenvalue for **AC2**. Bottom - NCI isosurface for **AC2** generated for $s=0.5$ a.u. with a blue-green-red color scale according to the values of $\text{sign}(\lambda_2)\rho$ from -0.05 to $+0.05$ a.u.

References

- (1) Pate, B. H.; Lehmann, K. K.; Scoles, G. *J. Chem. Phys.* **1991**, *95*, 3891 – 3916.